Uptake and metabolism of plasma-derived erucic acid by rat brain

Mikhail Y. Golovko* **and Eric J. Murphy**[1,*,†]

Department of Pharmacology, Physiology, and Therapeutics* and Department of Chemistry,† University of North Dakota, Grand Forks, ND 58202-9037

Abstract **We examined the ability of erucic acid (22:1n-9) to cross the blood-brain barrier (BBB) by infusing [14–^{14}C]22:1n-9 (170 μCi/kg, iv and icv) into awake, male rats. [1-^{14}C]arachidonic acid (20:4n-6) [intravenous (i.v.)] was the positive control. After i.v. infusion, 0.011% of the plasma [14-^{14}C]22:1n-9 was extracted by the brain, compared with 0.055% of the plasma [1-^{14}C]20:4n-6. The [14-^{14}C]22:1n-9 was extensively β-oxidized (60%), compared with 30% for [1-^{14}C]20:4n-6. Although 20:4n-6 was targeted primarily to phospholipid pools, 22:1n-9 was targeted to cholesteryl esters, triglycerides, and phospholipids. When [14-^{14}C]22:1n-9 was infused directly into the fourth ventricle of the brain [intracerebroventricular (i.c.v.)] for 7 days, 60% of the tracer entered the phospholipid pools, similar to the distribution observed for [1-^{14}C]20:4n-6. This demonstrates plasticity in the ability of the brain to esterify 22:1n-9 in an exposure-dependent manner. In i.v. and i.c.v. infused rats, a significant amount of tracer found in the phospholipid pools underwent sequential rounds of chain shortening and was found as [12-^{14}C]20:1n-9 and [10-^{14}C]oleic acid. These results demonstrate for the first time that intact 22:1n-9 crosses the BBB, is incorporated into specific lipid pools, and is chain-shortened.**—Golovko, M. Y., and E. J. Murphy. **Uptake and metabolism of plasma-derived erucic acid by rat brain.** ***J. Lipid Res.*** **2006.** 47: **1289–1297.**

Supplementary key words arachidonic acid • blood-brain barrier • adrenoleukodystrophy • fatty acid • fatty acid uptake

X-linked adrenoleukodystrophy (X-ALD; Online Mendelian Inheritance in Man 300100) has multiple phenotypes and is characterized by adrenal insufficiency and central nervous system demyelination (1). The biochemical hallmark of X-ALD is a marked increase in the amount of very long-chain saturated fatty acids (VLCFAs), often hexacosanoic acid (26:0), in plasma (2, 3), adrenal tissue, and brain (3, 4). Brain cholesteryl ester containing 26:0 is also increased in X-ALD subjects (3), as is cholesteryl ester mass (5, 6). The increase in cholesteryl esters results in reductions in cholesterol and sphingomyelin (6). These changes in lipid content are associated with a robust inflammatory response in the area surrounding the lesions, but not in nonpathologically involved brain regions (6). Changes in myelin phospholipids, free cholesterol, or perhaps an increase in free 26:0 intercalated into the membrane (7) may account for the demyelination observed in X-ALD.

The underlying mechanism accounting for the increase in tissue and plasma 26:0 is the decrease in peroxisomal β-oxidation of lignoceric acid (24:0), permitting its subsequent elongation to 26:0 (8–12). Unlike palmitic acid, 24:0 must be activated by the formation of its CoA derivative to cross the peroxisomal membrane (13); however, lignoceryl-CoA synthetase activity is reduced in X-ALD, resulting in limited activation of 24:0 (8, 9). In peroxisomes isolated from X-ALD-derived fibroblasts, exogenously provided 24:0-CoA is readily oxidized by peroxisomal β-oxidation, indicating that peroxisomal β-oxidation is intact (8). Furthermore, peroxisomal function in X-ALD fibroblasts is normal with regard to arachidonic acid (20:4n-6) β-oxidation and docosahexaenoic acid (22:6n-3) synthesis (14), indicating that peroxisomal function remains primarily intact.

Using positional cloning, lignoceryl-CoA ligase was found to be genetically unaltered in X-ALD, but a 75 kDa ABC cassette protein, adrenoleukodystrophy protein (ALDP; encoded for by *Abcd1*), was genetically altered (15–18). ALDP is an integral peroxisomal membrane protein (19), with immunoreactivity absent in nearly 70% of all X-ALD patients, and it is mutated in all patients examined (20, 21). Expression of either ALDP or related proteins in fibroblasts isolated from X-ALD patients increases 24:0 β-oxidation and markedly reduces 26:0 levels to control values (22–26). In addition to mutations in *Abcd1*, expression of *Abcd4* and *Bg1*, genes encoding for a peroxisomal membrane transporter protein and a VLCFA acyl-CoA synthetase, respectively, is reduced in normal white matter from X-ALD patients and

Abbreviations: 18:1n-9, oleic acid; 20:4n-6, arachidonic acid; 22:1n-9, erucic acid; 24:0, lignoceric acid; 26:0, hexacosanoic acid; ALDP, adrenoleukodystrophy protein; BBB, blood-brain barrier; i.c.v., intracerebroventricular; i.v., intravenous; LO, Lorenzo's Oil; VLCFA, very long-chain saturated fatty acid; X-ALD, X-linked adrenoleukodystrophy.

[1] To whom correspondence should be addressed.
e-mail: emurphy@medicine.nodak.edu

Manuscript received 18 January 2006 and in revised form 7 March 2006.
Published, JLR Papers in Press, March 8, 2006.
DOI 10.1194/jlr.M600029-JLR200

is associated with the early pathogenesis and severity of disease progression (27). Thus, the mutations in *Abcd1* as well as the decreased expression of *Abcd4* and *Bg1* account for the tissue accumulation of 26:0 in X-ALD.

Several mouse models for X-ALD have been established by ablating *Abcd1* in mice. These gene-ablated mice have decreased 24:0 β-oxidation in fibroblasts and increased levels of 26:0 in plasma and tissue, similar to those observed in X-ALD (28, 29). In these mice, the level of plasma cholesterol is increased and a high dietary intake of cholesterol exacerbates VLCFA accumulation (30). Although these mice have the biochemical characteristics of X-ALD, they lack the robust demyelination observed with this disease. Rather, the aged, gene-ablated mice demonstrate signs of adrenomyeloneuropathy (31), a much milder adult form of the disease associated with progressive demyelination in the spinal cord. The lack of central demyelination in these mice may indicate a greater gene redundancy in mice compared with humans, suggesting that proteins related to ALDP may partially replace the lost ALDP function in these gene-ablated mice (32).

Lorenzo's oil therapy was devised after the observation that X-ALD fibroblasts incubated with monoenoic fatty acids have reduced 26:0 levels (33), presumably by competing with saturated fatty acids in the elongation pathway (10, 11). Dietary restriction of saturated fatty acid intake and ingestion of gycerol trioleate only moderately reduced plasma 26:0 levels (34, 35). Subsequent studies included glycerol trierucate in a treatment regimen referred to as Lorenzo's Oil (LO) (U.S. Patent number 5,331,009). This treatment normalized plasma 26:0 levels within 4 weeks but did not halt neurological deterioration in patients with advanced X-ALD (36–38). Postmortem analysis of tissue from these X-ALD patients treated with LO show that erucic acid (22:1n-9) was absorbed from the gut and found esterified into liver, adrenal glands, and adipose lipid pools, but brain levels of 22:1n-9 were not different between treatment groups (39, 40). These results agree with the postmortem analysis from a single patient (36) and experiments in vivo showing that dietary monoenoic fatty acids do not alter mouse brain fatty acid composition (41). The lack of increased 22:1n-9 in brains from treated X-ALD patients suggests limited uptake into the central nervous system, perhaps as a result of poor movement of 22:1n-9 across the blood-brain barrier (BBB). A recent trial contradicts the supposition that LO is not effective, as it demonstrates that LO reduces clinical symptoms of X-ALD when administered early in life (42–44). This suggests that prolonged exposure to LO is clinically beneficial, although this clinical trial does not indicate that 22:1n-9 crosses the BBB; rather, it suggests that 22:1n-9 in the diet is beneficial in reducing 26:0 in the plasma.

The proposed mechanism of action for LO is supported by experiments in *Drosophila*, in which there is an ortholog to the mammalian microsomal very long-chain acyl-CoA synthetase (45). When this protein is mutated, it results in an increase in VLCFA and an age-dependent degeneration of the optic lobes, which is prevented by feeding LO to the flies (46). This also supports the human clinical trial indicating that dietary intake of LO limits the onset of neurological symptoms in afflicted boys.

LO dietary therapy has demonstrated in a number of clinical trials efficacy in ameliorating peripheral VLCFA levels associated with X-ALD and now demonstrates strong potential in limiting central nervous system demyelination (42–44). Yet, the question regarding the uptake of 22:1n-9 in the brain and its subsequent metabolism and deposition into brain lipid compartments remains unanswered. To address this question, we infused rats intravenously (i.v.) with [14-^{14}C]22:1n-9 and measured brain fatty acid uptake, deposition, and metabolism. In a parallel set of rats, we infused the [14-^{14}C]22:1n-9 directly into the brain and examined its metabolism and deposition into brain lipids. [1-^{14}C]20:4n-6 was used as a positive control (47–50). Here, we demonstrate for the first time that [14-^{14}C]22:1n-9 is taken up by the brain and esterified into brain lipid compartments. Direct infusion of [14-^{14}C]22:1n-9 alters the targeting, with more tracer found esterified in the phospholipid pools, suggesting that prolonged brain exposure alters the targeting of this fatty acid, consistent with the study demonstrating that early treatment with LO is clinically beneficial (42–44). In either infusion paradigm, brain [14-^{14}C]22:1n-9 was partially metabolized to [12-^{14}C]20:1n-9 and then to [10-^{14}C]oleic acid (18:1n-9).

METHODS

Animals

Male Sprague-Dawley rats (150–200 g) were obtained from Charles River Laboratories (St. Louis, MO) and maintained on standard laboratory rat chow and water ad libitum. This study was conducted in accordance with the National Institutes of Health Guidelines for the Care and Use of Laboratory Animals (publication 80-23) and under an animal protocol approved by the IACUC at the University of North Dakota (protocol 0010-1).

Rat surgery

After a rat was anesthetized with halothane (1–3%), the femoral artery and vein were catheterized with polyethylene tubing (PE-50). The wound area was anesthetized with xylocaine (1%) and closed using standard surgical staples. The hindquarters of the rat were placed in a plaster body cast, and the rat was taped loosely to a wooden block and maintained postoperatively in a temperature-controlled environment for 3–4 h.

Tracer preparation

The [14-^{14}C]22:1n-9 was custom synthesized by Moravek Biochemical (Brea, CA), and the structure and position of the ^{14}C was confirmed by the manufacturer using NMR and mass spectral analysis. The [1-^{14}C]20:4n-6 was also purchased from Moravek. Infusate was prepared by taking an aliquot of tracer in ethanol and evaporating the ethanol under a constant stream of N_2 at 50°C. Before use, radiotracer purity was assessed by gas-liquid chromatography and found to be >97% pure for [1-^{14}C]20:4n-6 and >92% pure for [14-^{14}C]22:1n-9. The fatty acid tracer was solubilized in 5 mM HEPES (pH 7.4) buffer containing "essentially fatty acid-free" BSA (50 mg/ml; Sigma Chemical Co., St. Louis, MO). Solubilization was facilitated by sonication in a bath sonicator for 45 min at 45°C. Radioactivity was determined using

liquid scintillation counting and adjusted to 100 μCi/ml. The appropriate amount of radiotracer was prepared for each rat using the infusion dose of 170 μCi/kg (51).

Infusion (i.v.)

Awake, adult male rats were infused with 170 μCi/kg [14-^{14}C] 22:1n-9 or [1-^{14}C]20:4n-6 into the femoral vein over 10 min using a constant-rate infusion paradigm to achieve steady-state plasma radioactivity. Before and during the experimental period, arterial blood samples (200 μl) were taken to determine plasma radioactivity. After infusion, the rat was euthanized using pentobarbital (100 mg/kg iv). Its brain was rapidly removed and frozen in liquid nitrogen. The time from pentobarbital injection to freezing was 35 ± 10 s. The tissue was stored at −80°C until used.

Plasma extraction

Arterial blood samples, taken at fixed times during the infusion period, were stored for up to 10 min on ice before separating the plasma by centrifugation with a Beckman Instruments microfuge (Fullerton, CA). Plasma lipids were then extracted by transferring a 100 μl aliquot of plasma into a tube containing 2 ml of chloroform-methanol (2:1, v/v), then mixing it by vortexing (52). The addition of 0.4 ml of 0.9% KCl to these tubes resulted in two phases. These phases were thoroughly mixed and then separated overnight in a −20°C freezer. The upper phase was removed, and the lipid-containing lower phase was rinsed with 0.43 ml of theoretical upper phase, consisting of chloroform-methanol-water (3:48:47, v/v), to remove any aqueous soluble contaminants (52). The upper phase was discarded, and a portion of the lower phase was dried and its radioactivity quantified using an LS5000 CE liquid scintillation counter (Beckman Instruments).

Blood extraction

Using the same procedure described above for plasma, whole blood was extracted to correct for residual blood radioactivity left in the tissue. For the brain, the residual blood was estimated at 2% (50, 53, 54).

Infusion (intracerebroventricular)

For intracerebroventricular (i.c.v.) infusion, the rat was anesthetized with pentobarbital and mounted in a stereotaxic frame, with the incisors set 3.3 mm dorsal to the earbars. The skull was exposed, a small hole was drilled through the skull at 2.5 mm caudal to lambda at the midline, and an 8 mm long cannula was inserted 7.5 mm ventral from the dura into the fourth ventricle. Coordinates and perfusion of the brain's ventricles were confirmed in a separate set of rats by infusing dye and examining dye distribution postmortem. The infusate was prepared in sterile artificial saline containing essentially fatty acid-free BSA and [14-^{14}C]22:1n-9 (170 μCi/kg) under sterile conditions. An osmotic minipump was placed in the subscapular region, and the fatty acid was infused over a 7 day period.

Tissue lipid extraction

Frozen tissue was pulverized under liquid nitrogen temperatures. Lipids from tissue powder were extracted in a Tenbroeck tissue homogenizer using a two-phase system (52). Briefly, the tissue mass (grams) was multiplied by a correction factor of 1.28 to convert it to an equivalent value expressed in milliliters (55). This value represents 1 volume. The pulverized tissue was placed in the homogenizer, and 17 volumes of chloroform-methanol (2:1, v/v) was added. Tissue was homogenized until there was a fine particulate-like suspension. The solvent was removed, and the homogenizer was rinsed with 3 volumes of chloroform-methanol (2:1, v/v). The rinse was added to the original sample, and 4 volumes of 0.9% KCl solution was added to this combined lipid extract. After vigorous mixing, phase separation was facilitated by centrifugation. The upper aqueous phase and proteinaceous interface was removed and saved in a 20 ml glass scintillation vial. The lower organic phase was washed twice with 2 ml of theoretical upper phase, with phase separation facilitated by centrifugation between washes. The washes were removed and combined with the previously removed upper phase. The washed lower phase was dried under a stream of nitrogen, and the lipids were redissolved in 3 ml of *n*-hexane-2-propanol (3:2, v/v) containing 5.5% water.

Aqueous fraction

Radioactivity in the aqueous fraction from the tissue extraction, including the theoretical upper phase from the two wash steps, was measured using liquid scintillation counting. Radioactivity was determined after the addition of 10 ml of Scintiverse II BD (Fisher Scientific, Pittsburgh, PA) using an LS5000 CE liquid scintillation counter (Beckman Instruments). The addition of the aqueous material to the scintillation cocktail did not adversely affect the counter efficiency.

Thin-layer chromatography

Phospholipids and neutral lipids were separated by TLC. For each separation, 100 μl of sample was spotted onto a TLC plate. Phospholipids were separated on heat-activated Whatman silica gel-60 plates (20 × 20 cm, 250 μm) developed in chloroform-methanol-acetic acid-water (60:30:3:1, v/v). This solvent system resolves cardiolipin, phosphatidic acid, and ethanolamine glycerophospholipids but not phosphatidylinositol and phosphatidylserine. Phosphatidylserine and phosphatidylinositol were resolved using heat-activated Whatman silica gel-60 plates (20 × 20 cm, 250 μm) and developed in chloroform-methanol-acetic acid-water (50:37.5:3.5:2, v/v) (56). Neutral lipids were separated using heat-activated silica G plates (Analtech, Newark, DE) developed in petroleum ether-diethyl ether-acetic acid (70:30:1.3, v/v) (57). This solvent system resolves cholesterol, cholesteryl esters, diacylglycerols, nonesterified fatty acids, and triacylglycerols. Lipid fractions were identified using authentic standards (Doosan-Serdary, Englewood Cliffs, NJ, and NuChek Prep, Elysian, MN).

Analysis of [14-^{14}C]22:1n-9 metabolism in plasma and brain

Plasma and brain lipid extracts were fractionated into neutral lipid and phospholipid fractions using silicic acid column chromatography (Clarkson Chemical Co., Inc., Williamsport, PA) (58). Fatty acids were separated and quantified after conversion to their corresponding phenacyl esters (59, 60). Briefly, an aliquot of lipid extract was subjected to saponification at 100°C for 30 min in 2% KOH in ethanol, which was then acidified with hydrochloric acid. The released fatty acids were extracted with hexane, and phenacyl esters were then prepared by the addition of acetone containing 2-bromoacetophenone (10 mg/ml) (Sigma) and triethylamine (10 mg/ml) followed by incubation at 100°C for 5 min. After the addition of acetic acid (2 mg/ml), the samples were incubated for another 5 min. Tripentadecanoin (NuChek Prep) was used as the internal standard.

Individual fatty acid phenacyl esters were separated by HPLC on a C-18(2) Luna column (Phenomenex, Torrance, CA). The HPLC system was controlled by a Beckman Instruments 127 solvent module. We modified an existing HPLC method (60) to resolve VLCFA using a binary solvent system (A, water; B, aceto-

nitrile). The flow rate was 1 ml/min, and the initial percentage of B was 80%. At 310 min, the percentage of B was increased to 90% over 1 min, and at 490 min, it was increased to 96% over 1 min. At 550 min, the percentage of B was returned to 80% over 1 min. The eluent was monitored at 242 nm using a Beckman 166 ultraviolet/visible light detector. Fatty acids were quantified using a standard curve from commercially purchased standards (NuChek Prep), and Pentadecanoic acid was the internal standard. Peaks corresponding to individual fatty acid phenacyl esters were collected, and radioactivity was determined by liquid scintillation counting using an LS5000 CE liquid scintillation counter (Beckman Instruments).

Liquid scintillation counting

Bands corresponding to the appropriate lipid fractions were scraped into 20 ml liquid scintillation vials, and 0.5 ml of water was added followed by 10 ml of Scintiverse BD (Fisher Scientific). After mixing, the samples were allowed to stabilize for at least 1 h before being quantified by liquid scintillation counting.

Statistics

Statistical analysis was done using Instat2 from GraphPad (San Diego, CA). Statistical significance was assessed using Student's *t*-test or one-way ANOVA coupled with the Tukey-Kramer posttest where appropriate, with $P < 0.05$ considered significant. n is defined as the number of rats in a group.

RESULTS

Plasma curves

The plasma curves for [14-^{14}C]22:1n-9 and [1-^{14}C]20:4n-6 rats are shown in **Fig. 1**. The integrated area under the curve for each plasma curve was calculated with Sigma Plot using the trapezoidal rule. For [14-^{14}C]22:1n-9-infused rats, the average integrated plasma curve area was 2,281 ± 835 (n = 6), whereas for [1-^{14}C]20:4n-6-infused rats, the average integrated plasma curve area was 2,013 ± 378 (n = 6). These average areas were not significantly different between the groups.

Although [1-^{14}C]20:4n-6 is minimally metabolized in the plasma during the infusion (61), it is unknown whether plasma [14-^{14}C]22:1n-9 undergoes significant metabolism. In plasma, >91% of the infused tracer was found as 22:1n-9, with only minimal amounts of fatty acids (<1%) derived by chain elongation or shortening of the [14-^{14}C]22:1n-9 (**Table 1**). However, we did find 6.5% of the tracer associated with stearic acid, with only minimal amounts (<1%) chain-elongated or -shortened. Because the [14-^{14}C]22:1n-9 was minimally metabolized into other n-9 family fatty acids, it is unlikely that the 18:0 represents recycled carbon, especially with only 0.3% in palmitic acid; rather, it more likely represents a contaminant in the custom-synthesized tracer.

Brain uptake and distribution of 22:1n-9

Rats were infused with [14-^{14}C]22:1n-9 (i.v.) to determine whether this fatty acid readily crossed the BBB, and to assess its incorporation into brain lipid pools, two separate infusion paradigms, i.v. and i.c.v., were used. Uptake and incorporation into the brain was compared with the uptake and incorporation of infused [1-^{14}C]20:4n-6 (i.v.). For i.v. infused fatty acids, uptake was corrected for residual blood remaining in the tissue, as described in Methods. The amount of tracer extracted from the dose given for each infusion paradigm and fatty acid was calculated based upon the dose given to each individual rat. The percentages of the dose extracted by the brain were 0.011 ± 0.004% for plasma-derived [14-^{14}C]22:1n-9 (i.v.), 0.055 ± 0.009% for plasma-derived [1-^{14}C]20:4n-6 (i.v.), and 0.078 ± 0.016% for [14-^{14}C]22:1n-9 (i.c.v.). The amount of tracer (nCi/g wet weight) found in the total, aqueous, and organic fractions was also determined (**Fig. 2**). Although equal doses

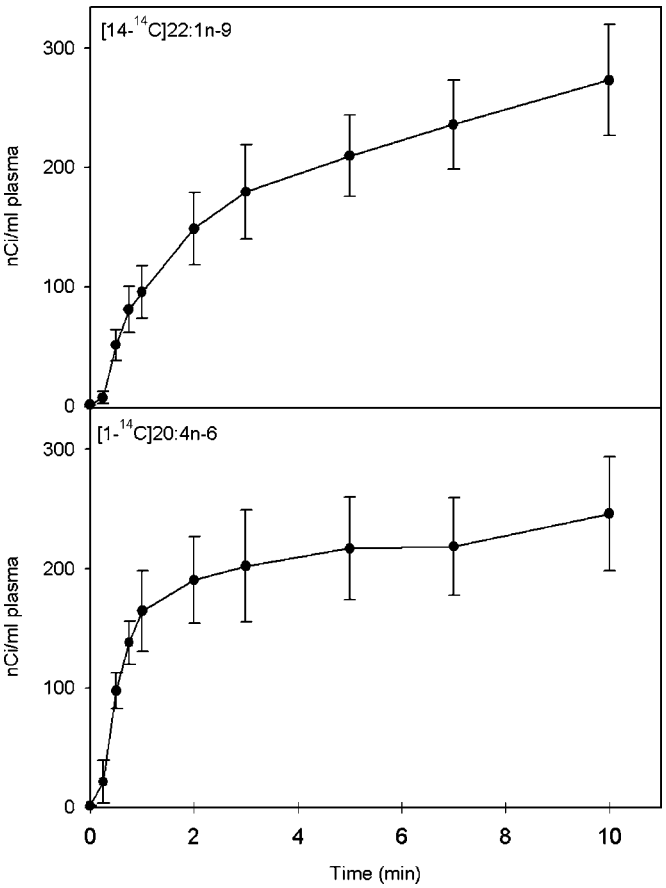

Fig. 1. Plasma curves for [14-^{14}C]erucic acid- (22:1n-9) and [1-^{14}C]arachidonic acid- (20:4n-6) infused rats. Infusions were done as described in Methods. Values are means ± SD (n = 6).

TABLE 1. Distribution of tracer radioactivity among plasma fatty acids

Fatty Acid	Percentage Distribution of Radioactivity
16:0 Palmitic acid	0.3 ± 0.1
18:0 Stearic acid	6.5 ± 1.9
18:1n-9 Oleic acid	0.3 ± 0.1
20:0 Arachidic acid	0.3 ± 0.1
20:1n-9 Eicosenoic acid	0.4 ± 0.2
22:1n-9 Erucic acid	91.4 ± 2.0
22:0 Behenic acid	0.3 ± 0.1
24:0 Lignoceric acid	0.7 ± 0.3
24:1n-9 Nervonic acid	0.2 ± 0.1

Values represent means ± SD (n = 6).

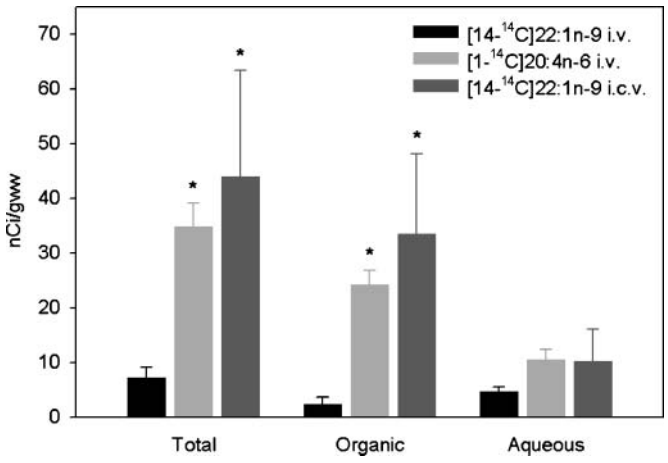

Fig. 2. Brain uptake of infused [14-^{14}C]22:1n-9 [intravenous (i.v.) or intracerebroventricular (i.c.v.)] and [1-^{14}C]20:4n-6 (i.v.) was assessed as described in Methods. For each infusion paradigm, the dosage was 170 μCi/kg. For i.v. infusion, the duration of infusion was 10 min, whereas for i.c.v. infusion, the duration was 7 days. Values are means ± SD (n = 6). * Significantly different from [14-^{14}C]22:1n-9 (i.v.) ($P < 0.05$). gww, gram wet weight.

were administered to the rats, 4.7-fold more [1-^{14}C]20:4n-6 entered the brain compared with [14-^{14}C]22:1n-9 (i.v), although when an equal dose of [14-^{14}C]22:1n-9 was infused i.c.v. directly into the brain, there was no difference between the two fatty acids. No differences in the amount of tracer found in the aqueous fraction were observed between groups, although significantly more tracer was found in the organic fraction for rats infused i.v. with [1-^{14}C]20:4n-6 or infused i.c.v. with [14-^{14}C]22:1n-9 compared with [14-^{14}C]22:1n-9.

Distribution of tracer into the organic or aqueous fractions was also determined (**Fig. 3**). For [14-^{14}C]22:1n-9 infused i.v., there was a marked increase in the distribution of tracer in the aqueous fraction relative to [1-^{14}C]20:4n-6 (i.v.) or [14-^{14}C]22:1n-9 (i.c.v.). In contrast, the distribution of tracer into the organic fraction was reduced in rats infused with [14-^{14}C]22:1n-9 (i.v.) relative to [1-^{14}C]20:4n-6 (i.v.) or [14-^{14}C]22:1n-9 (i.c.v.). These data demonstrate the robust use of plasma-derived [14-^{14}C]22:1n-9 for β-oxidation compared with the long-term exposure of [14-^{14}C]22:1n-9 via i.c.v. infusion, for which the fatty acid was β-oxidized to a similar extent as plasma-derived [1-^{14}C]20:4n-6 (i.v.).

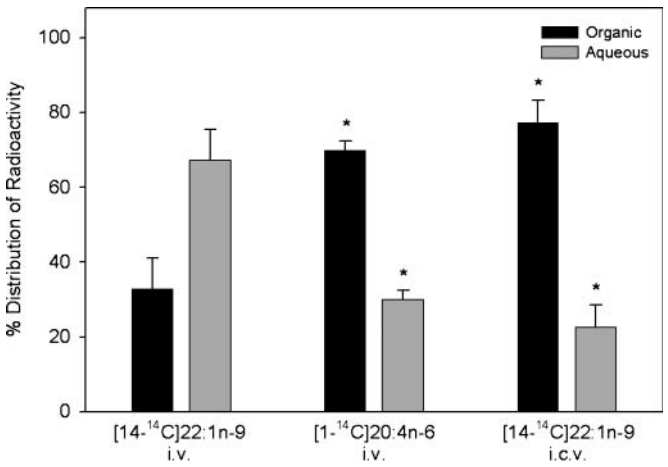

Fig. 3. Distribution of infused [14-^{14}C]22:1n-9 (i.v. or i.c.v.) and [1-^{14}C]20:4n-6 (i.v.) in organic and aqueous fractions from extracted brain tissue. Values are means ± SD (n = 6). * Significantly different from [14-^{14}C]22:1n-9 (i.v.) ($P < 0.05$).

Distribution of radiotracers in brain lipid pools

Tracer distribution into brain lipid pools was also determined (**Fig. 4**). Very little of the infused [14-^{14}C]22:1n-9 (i.v.) was incorporated into the phospholipid fraction compared with either the [14-^{14}C]22:1n-9 (i.c.v.) or [1-^{14}C]20:4n-6 (i.v.). However, when infused directly into the brain, [14-^{14}C]22:1n-9 was found in the phospholipid fraction nearly 3-fold more than when infused i.v.; although this distribution was less than for [1-^{14}C]20:4n-6, it was more similar to [1-^{14}C]20:4n-6 than it was to [14-^{14}C]22:1n-9 infused i.v. In addition, much more [14-^{14}C]22:1n-9 was found in the cholesteryl ester fraction or in the FFA fraction, regardless of the infusion paradigm, relative to [1-^{14}C]20:4n-6. These results demonstrate that the incorporation of [14-^{14}C]22:1n-9 into brain lipid fractions occurs, although in a manner that was significantly distinct from [1-^{14}C]20:4n-6, indicating that the brain does not esterify these two fatty acids into lipid pools in a similar manner. Nonetheless, constant exposure of the brain to 22:1n-9 significantly altered its targeting, suggesting some degree of plasticity in the fatty acid-targeting mechanism(s) in the brain.

Metabolism of [14-^{14}C]22:1n-9 in the brain

To determine whether the infused [14-^{14}C]22:1n-9 was chain-elongated or -shortened, we determined the distribution of radioactivity found in other fatty acids (**Fig. 5**). In both i.v. and i.c.v. infused rats, the bulk of the tracer was

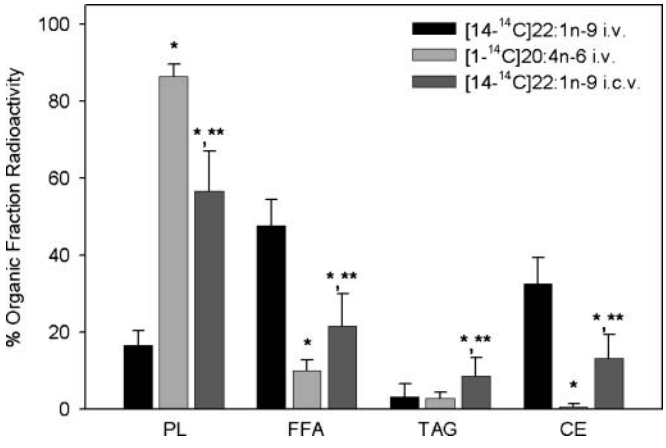

Fig. 4. Distribution of infused [14-^{14}C]22:1n-9 (i.v. or i.c.v.) and [1-^{14}C]20:4n-6 (i.v.) in different brain lipid fractions. Values are means ± SD (n = 6). * Significantly different from [14-^{14}C]22:1n-9 (i.v.) ($P < 0.05$). ** Significantly different from [1-^{14}C]20:4n-6 (i.v.) ($P < 0.05$). CE, cholesteryl ester; PL, phospholipid; TAG, triacylglycerol.

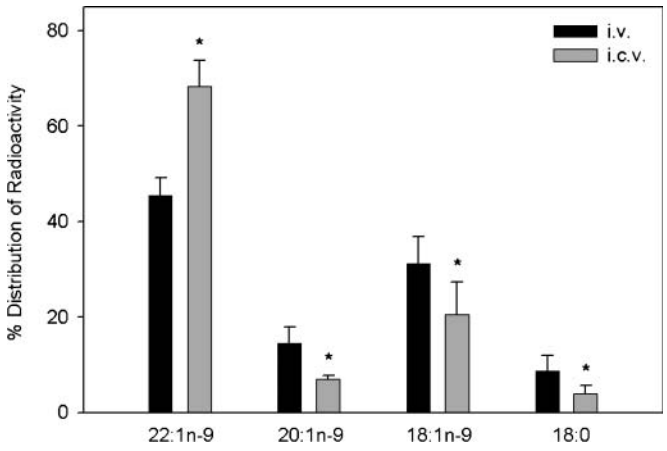

Fig. 5. Distribution of infused [14-^{14}C]22:1n-9 (i.v. or i.c.v.) among different n-9 family fatty acids, demonstrating the metabolism of the tracer via chain shortening. Values are means ± SD (n = 6). * Significantly different from [14-^{14}C]22:1n-9 (i.v.) ($P < 0.05$). 18:1n-9, oleic acid.

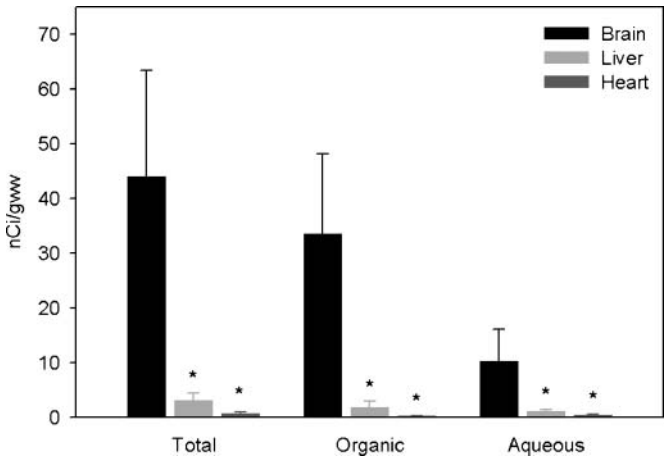

Fig. 6. Uptake of infused [14-^{14}C]22:1n-9 (i.c.v.) into brain, liver, or heart, demonstrating the limited movement of tracer infused i.c.v. into other tissues. Values are means ± SD (n = 6). * Significantly different from brain ($P < 0.05$). gww, gram wet weight.

found as [14-^{14}C]22:1n-9, with [12-^{14}C]20:1n-9 appearing to be an intermediate pool. The terminal pool was found to be [10-^{14}C]18:1n-9, of which ~25% of the tracer was found. Similar to the results for plasma, there was a small amount of radioactive 18:0 found in the brain, with a magnitude similar to that observed in plasma. We did not observe the elongation of [14-^{14}C]22:1n-9 to [16-^{14}C]24:1n-9 in either the i.v. or i.c.v. infused rats. Thus, infused [14-^{14}C]22:1n-9 undergoes a significant amount of metabolism within the brain compartment that does not represent incorporation of these radioactive fatty acids from the plasma, as they were found in the plasma only in trace amounts (<1%).

Loss of [14-^{14}C]22:1n-9 to other tissue compartments

To determine whether infused [14-^{14}C]22:1n-9 (i.c.v.) remained primarily in the brain, we analyzed the incorporation of this tracer or its metabolites into the liver and heart organic and aqueous fractions (**Fig. 6**). When infused i.c.v., the bulk of the infused tracer remained in the brain compartment, with very little incorporated into the liver or heart.

DISCUSSION

Although there are other potential therapies for X-ALD, including treatment with lovastatin (62, 63) and 4-phenylbutyrate (32), only LO and bone marrow transplantation are effective treatments that preserve central nervous system myelin and neurological function in boys afflicted with X-ALD (1, 42, 43). Recent studies demonstrate that the use of LO in patients is effective (42, 43), but only in patients without neurological involvement (64). In patients with neurological symptoms, bone marrow transplantation has proven to be successful (1).

In patients with X-ALD, LO rapidly normalizes plasma VLCFA and effectively reduces tissue levels of VLCFA, except in the brain (36–40). These early, limited clinical trials suggested that 22:1n-9, the active component of LO, failed to cross the BBB (36, 39, 40), thereby accounting for the lack of efficacy in limiting the rapid progression of the demyelination in these patients. However, lack of an increase in steady-state fatty acid levels is not sufficient evidence to discount the ability of 22:1n-9 to cross the BBB. To address this question, we infused rats with [14-^{14}C]22:1n-9 and measured its metabolism and incorporation into brain lipid compartments. In a parallel set of rats, we infused [1-^{14}C]20:4n-6 as a positive control because of its well-known ability to cross the BBB and to be incorporated into brain lipid compartments (47–50).

It is important to note that in this study we measured the ability of albumin-bound [14-^{14}C]22:1n-9 to enter the brain, rather than the entry of tracer infused in a triglyceride form, such as that used in LO. This was done for four reasons. First, others have demonstrated that dietary 22:1n-9 provided in triglyceride form enters the blood and tissues, including the brain (65, 66). This was further demonstrated in early studies using LO, in which fatty acid accumulation in a number of tissues was demonstrated (39, 40). Second, upon digestion of LO, the free fatty acids and monoacylglycerol will enter the enterocyte, where these components will be used to form triacylglycerides and phospholipids, as demonstrated by the dietary uptake studies. Hence, there will be a rearrangement of the components into other molecular species that will be exported into the circulation. Third, at the level of tissues, including the brain, these triglycerides are cleaved by lipoprotein lipase, thereby releasing the free fatty acid (67). In addition, under physiological conditions, fatty acids are also bound to albumin for transport (67). Fourth, in heart, the infusion of either triglyceride or free fatty acid complexed with albumin does not affect the kinetics of tracer movement from the plasma into the heart (68–70). The rapid interchange of fatty acids hydrolyzed from triglycerides with the free fatty acid pool negates any difference between

these two routes of entry with regard to the kinetics of fatty acid uptake (69). Similar expectations are that the brain has a similar inability to distinguish between these two forms of fatty acid delivery to the brain (67). Thus, here, we model the physiological process for fatty acid entry into brain using tracer complexed with albumin to determine the uptake of 22:1n-9 into the brain.

We clearly demonstrate, using an established infusion paradigm (47–50), that 22:1n-9 crossed the BBB and was found in brain metabolic compartments. Although we could not detect an alteration of plasma concentrations of 22:1n-9 during infusion (data not shown), the continuing increase in the plasma curve suggests that the plasma steady-state content of 22:1n-9 was not achieved during the infusion (Fig. 1), suggesting an undetected perturbation of plasma 22:1n-9 mass. This was not the case for 20:4n-6, as it achieved steady state in the plasma. Nonetheless, these data clearly demonstrate that the magnitude of 20:4n-6 uptake was only 5-fold greater than that for 22:1n-9, indicating that brain has a greater preference for the uptake of 20:4n-6 over 22:1n-9. In addition, once in the brain, significant amounts of [14-^{14}C]22:1n-9 were found to be chain-shortened (Fig. 5), whereas 20:4n-6 is minimally chain-shortened or -elongated (61). These two points, limited uptake and the rapid chain shortening of 22:1n-9 upon entry, may account for the lack of an increase in brain steady-state 22:1n-9 levels in early clinical trials compared with other tissues (36, 39, 40).

Once 22:1n-9 entered the brain, it was found distributed in the organic and aqueous fractions. Compared with 20:4n-6, much more 22:1n-9 was found in the aqueous fraction, representing β-oxidation, suggesting a differential targeting of these two fatty acids into brain metabolic pools (Fig. 3). Introduction of [14-^{14}C]22:1n-9 into the fourth ventricle, using a continuous infusion paradigm, resulted in a dramatic shift in the targeting of tracer (Fig. 4). Under these conditions, the brain esterified nearly 60% of the tracer into brain phospholipids, with a significant reduction in the amount targeted to cholesteryl ester or left in the FFA pool. Overall, the constant infusion of [14-^{14}C]22:1n-9 resulted in a dramatic shift in the distribution of tracer in brain lipid compartments, more closely resembling the distribution of infused [1-^{14}C]20:4n-6 (i.v.) than the distribution of infused [14-^{14}C]22:1n-9 (i.v.). This change in the distribution of [1-^{14}C]22:1n-9 suggests a degree of plasticity in the esterification of this fatty acid into brain lipid pools. However, it is important to note that, regardless of the route of entry, the tracer was chain-shortened to a similar degree (Fig. 5), indicating that the increase in tracer found in the phospholipids was not merely an increase in a chain-shortened form of the tracer; rather, it demonstrates an increased ability of the brain to activate the 22:1n-9 to the 22:1n-9-CoA for esterification into brain lipid pools.

Others have demonstrated the ability of diet-derived 22:1n-9 to enter the brain (65, 66). However, in one of these studies, the form of the tracer was not identified (65), whereas the other only measured an increase in mass to assess incorporation (66). Neither of these studies examined the potential for the brain to metabolize 22:1n-9, either into longer or shorter chain n-9 family fatty acids. When absorbed through the diet, 22:1n-9 is increased primarily in the heart and adrenal glands (66), which is consistent with postmortem results from patients given LO (39, 40). Infusion of [2-^{14}C]22:1n-9 (i.v.) resulted in limited deposition into brain, which accounted for ~2% of the tracer measured in a number of tissues harvested 6.5 h after infusion via the tail vein (65), compared with 0.03% after dietary consumption of the same tracer (65). However, it is important to note that the form of the tracer was not determined in either of these experimental groups. Here, we determined the incorporation of tracer under steady-state infusion conditions and verified the incorporation of 22:1n-9 into brain and its subsequent metabolism via chain shortening.

It is important to note that we did not find any chain-elongated [14-^{14}C]22:1n-9. Because LO is thought to compete with endoplasmic reticulum-localized elongases, the lack of [16-^{14}C]24:1 in the brain suggest that the brain is ill-equipped to elongate this fatty acid. Clearly, this elongation occurs in other experimental paradigms in other tissues (10, 33, 39). In human fibroblasts, incubation with deuterium-labeled 18:1n-9 results in elongation to other n-9 family fatty acids, and this potential for elongation is increased in fibroblasts from X-ALD patients (12). In addition, treatment of patients with LO appears to enhance the elongation of 22:1n-9, demonstrating an apparent shift in the ability of fibroblasts from these patients to elongate fatty acids (12). However, even after the direct exposure of the brain to [14-^{14}C]22:1n-9 for 7 days, we did not observe any elongation to [16-^{14}C]24:1n-9, although the impact of X-ALD on this elongation was not determined using mouse models (28, 29). Nonetheless, we did not observe any increases in elongation of our tracer, indicating that under our experimental paradigm, in normal rats this process is extremely limited.

In summary, we demonstrate that 22:1n-9 readily crosses the BBB and is esterified into brain lipid compartments. These studies also demonstrate that the magnitude of uptake is similar to that of 20:4n-6, although the distribution among lipid compartments was much different between the two fatty acids. Constant infusion of [14-^{14}C]22:1n-9 into the fourth ventricle increased the amount of tracer esterified into lipid compartments and caused a shift in its distribution into phospholipid pools. Under these conditions, the distribution was similar to that observed for [1-^{14}C]20:4n-6 (i.v.), suggesting that during prolonged exposure, the brain demonstrates plasticity with regard to targeting 22:1n-9 to phospholipids. The tracer found in the brain was not accounted for by the entry of metabolized tracer, as the tracer was minimally metabolized in the plasma. However, within the brain, the tracer was chain-shortened to 18:1n-9, demonstrating the ability of the brain to effectively metabolize and esterify the altered tracer. Thus, 22:1n-9 crosses the BBB, and although the tracer was significantly esterified into brain lipid pools, it was found as either 22:1n-9 or its chain-shortened metabolites 20:1n-9 and 18:1n-9.

The authors thank Dr. Carole Haselton for her surgical efforts and technical skills used in the lipid analysis described herein and Mrs. Cindy Murphy for typing the manuscript. This work was supported by a grant from The Myelin Project to E.J.M. and in part by a project (E.J.M.) on a COBRE Grant from the National Institutes of Health 1P20 RR17699-01.

REFERENCES

1. Dubois-Dalcq, M., V. Feigenbaum, and P. Aubourg. 1999. The neurobiology of X-linked adrenoleukodystrophy, a demyelinating peroxisomal disorder. *Trends Neurosci.* **22:** 4–12.
2. Moser, H. W., A. B. Moser, K. K. Frayer, W. Chen, J. D. Schulman, B. P. O'Neill, and Y. Kishimoto. 1981. Adrenoleukodystrophy: increased plasma content of saturated very long chain fatty acids. *Neurology.* **31:** 1241–1249.
3. Igarashi, M., H. H. Schaumburg, J. Powers, Y. Kishimoto, E. Kolodny, and K. Suzuki. 1976. Fatty acid abnormality in adrenoleukodystrophy. *J. Neurochem.* **26:** 851–860.
4. Theda, C., A. B. Moser, J. M. Powers, and H. W. Moser. 1992. Phospholipids in X-linked adrenoleukodystrophy white matter: fatty acid abnormalities before the onset of demyelination. *J. Neurol. Sci.* **110:** 195–204.
5. Wilson, R., and J. R. Sargent. 1993. Lipid and fatty acid composition of brain tissue from adrenoleukodystrophy patients. *J. Neurochem.* **61:** 290–297.
6. Paintlia, A. S., A. G. Gilg, M. Khan, A. K. Signh, E. Barbosa, and I. Singh. 2003. Correlation of very long chain fatty acid accumulation and inflammatory disease progression in childhood X-ALD: implications for potential therapies. *Neurobiol. Dis.* **14:** 425–439.
7. Ho, J. K., H. Moser, Y. Kishimoto, and J. A. Hamilton. 1995. Interactions of a very long chain fatty acid with model membranes and serum albumin. *J. Clin. Invest.* **96:** 1455–1463.
8. Lazo, O., M. Contreras, M. Hashmi, W. Stanley, C. Irazu, and I. Singh. 1988. Peroxisomal lignoceroyl-CoA ligase deficiency in childhood adrenoleukodystrophy and adrenomyeloneuropathy. *Proc. Natl. Acad. Sci. USA.* **85:** 7647–7651.
9. Lazo, O., M. Contreras, A. Bhushan, W. Stanley, and I. Singh. 1989. Adrenoleukodystrophy: impaired oxidation of fatty acids due to peroxisomal lignoceroyl-CoA ligase deficiency. *Arch. Biochem. Biophys.* **270:** 722–728.
10. Wilson, R., D. R. Tocher, and J. R. Sargent. 1992. Effects of exogenous monounsaturated fatty acids on fatty acid metabolism in cultured skin fibroblasts from adrenoleukodystrophy patients. *J. Neurol. Sci.* **109:** 207–214.
11. Koike, R., S. Tsuji, T. Ohno, Y. Suzuki, T. Orii, and T. Miyatake. 1991. Physiological significance of fatty acid elongation system in adrenoleukodystrophy. *J. Neurol. Sci.* **103:** 188–194.
12. Kemp, S., F. Valianpour, S. Denis, R. Ofman, R-J. Sanders, P. Mooyer, P. G. Barth, and R. J. A. Wanders. 2005. Elongation of very long-chain fatty acids is enhanced in X-linked adrenoleukodystrophy. *Mol. Genet. Metab.* **84:** 144–151.
13. Singh, I., O. Lazo, G. S. Dhaunsi, and M. Contreras. 1992. Transport of fatty acids into human and rat peroxisomes. Differential transport of palmitic and lignoceric acids and its implication to X-adrenoleukodystrophy. *J. Biol. Chem.* **267:** 13306–13313.
14. Petroni, A., B. Bertagnolio, P. La Spada, M. Blasevich, N. Papini, S. Govoni, M. Rimoldi, and C. Galli. 1998. The β-oxidation of arachidonic acid and the synthesis of docosahexaenoic acid are selectively and consistently altered in skin fibroblasts from three Zellweger patients versus X-adrenoleukodystrophy, Alzheimer and control subjects. *Neurosci. Lett.* **250:** 145–148.
15. Mosser, J., A. M. Douar, C. O. Sarde, P. Kioschis, R. Feil, H. Moser, A. M. Poustka, J. L. Mandel, and P. Aubourg. 1993. Putative X-linked adrenoleukodystrophy gene shares unexpected homology with ABC transporters. *Nature.* **361:** 726–730.
16. Cartier, N., C. O. Sarde, A. M. Douar, J. Mosser, J. L. Mandel, and P. Aubourg. 1993. Abnormal messenger RNA expression and a missense mutation in patients with X-linked adrenoleukodystrophy. *Hum. Mol. Genet.* **2:** 1949–1951.
17. Aubourg, P., J. Mosser, A. M. Douar, C. O. Sarde, J. Lopez, and J. L. Mandel. 1993. Adrenoleukodystrophy gene: unexpected homology to a protein involved in peroxisome biogenesis. *Biochimie.* **75:** 293–302.
18. Douar, A. M., J. Mosser, C. O. Sarde, J. Lopez, J. L. Mandel, and P. Aubourg. 1994. X-linked adrenoleukodystrophy gene: identification of a candidate gene by positional cloning. *Biomed. Pharmacother.* **48:** 215–218.
19. Contreras, M., J. Mosser, J. L. Mandel, P. Aubourg, and I. Singh. 1994. The protein coded by the X-adrenoleukodystrophy gene is a peroxisomal integral membrane protein. *FEBS Lett.* **344:** 211–215.
20. Feigenbaum, V., G. Lombard-Platet, S. Guidoux, C. O. Sarde, J. L. Mandel, and P. Aubourg. 1996. Mutational and protein analysis of patients and heterozygous women with X-linked adrenoleukodystrophy. *Am. J. Hum. Genet.* **58:** 1135–1144.
21. Kemp, S., P. A. W. Mooyer, P. A. Bolhuis, B. M. van Geel, J. L. Mandel, P. G. Barth, P. Aubourg, and R. J. A. Wanders. 1996. ALDP expression in fibroblasts of patients with X-linked adrenoleukodystrophy. *J. Inherit. Metab. Dis.* **19:** 667–674.
22. Cartier, N., J. Lopez, P. Moullier, F. Ricchiccioli, M. O. Rolland, P. Jorge, J. Mosser, J. L. Mandel, P. F. Bougneres, O. Danos, et al. 1995. Retroviral-mediated gene transfer corrects very long chain fatty acid metabolism in adrenoleukodystrophy fibroblasts. *Proc. Natl. Acad. Sci. USA.* **92:** 1674–1678.
23. Shinnoh, N., T. Yamada, T. Toshimura, H. Furuya, Y. Yoshida, Y. Suzuki, N. Shimozawa, T. Orii, and T. Kobayashi. 1995. Adrenoleukodystrophy: the restoration of peroxisomal β-oxidation by transfection of normal cDNA. *Biochem. Biophys. Res. Commun.* **210:** 830–836.
24. Netik, A., S. Forss-Petter, A. Holzinger, B. Molzer, G. Unterrainer, and J. Berger. 1999. Adrenoleukodystrophy-related protein can compensate functionally for adrenoleukodystrophy protein deficiency (X-ALD): implications for therapy. *Hum. Mol. Genet.* **8:** 907–913.
25. Flavigny, E., A. Sanjah, P. Aubourg, and N. Cartier. 1999. Retroviral-mediated adrenoleukodystrophy-related gene transfer corrects very long chain fatty acid metabolism in adrenoleukodystrophy fibroblasts: implications for therapy. *FEBS Lett.* **448:** 261–264.
26. Braiterman, L. T., S. Zheng, P. A. Watkins, M. T. Geraghty, G. Johnson, M. C. McGuinness, A. B. Moser, and K. D. Smith. 1998. Suppression of peroxisomal membrane protein defects by peroxisomal ATP binding cassette (ABC) proteins. *Hum. Mol. Genet.* **7:** 239–247.
27. Asheur, M., I. Bieche, I. Laurendeau, A. Moser, B. Hainque, M. Vidaud, and P. Aubourg. 2005. Decreased expression of *ABCD4* and *BG1* genes early in the pathogenesis of X-linked adrenoleukodystrophy. *Hum. Mol. Genet.* **14:** 1293–1303.
28. Kobayashi, T., N. Shinnoh, A. Kondo, and T. Yamada. 1997. Adrenoleukodystrophy protein-deficient mice represent abnormality of very long chain fatty acid metabolism. *Biochem. Biophys. Res. Commun.* **232:** 631–636.
29. Lu, J. F., A. M. Lawler, P. A. Watkins, J. M. Powers, A. B. Moser, H. W. Moser, and K. D. Smith. 1997. A mouse model for X-linked adrenoleukodystrophy. *Proc. Natl. Acad. Sci. USA.* **94:** 9366–9371.
30. Weinhofer, I., S. Forss-Petter, M. Kunze, M. Zigman, and J. Berger. 2005. X-linked adrenoleukodystrophy mice demonstrate abnormalities in cholesterol metabolism. *FEBS Lett.* **579:** 5512–5516.
31. Pujol, A., C. Hindelang, N. Callizot, U. Bartsch, M. Schachner, and J. L. Mandel. 2002. Late onset neurological phenotype of the X-ALD gene inactivation in mice: a mouse model for adrenomyeloneuropathy. *Hum. Mol. Genet.* **11:** 499–505.
32. Kemp, S., H. M. Wei, J. F. Lu, L. T. Braiterman, M. C. McGuinness, A. B. Moser, P. A. Watkins, and K. D. Smith. 1998. Gene redundancy and pharmacological gene therapy: implications for X-linked adrenoleukodystrophy. *Nat. Med.* **4:** 1261–1268.
33. Rizzo, W. B., P. A. Watkins, M. W. Phillips, D. Cranin, B. Campbell, and J. Avigan. 1986. Adrenoleukodystrophy: oleic acid lowers fibroblast saturated C22-26 fatty acids. *Neurology.* **36:** 357–361.
34. Moser, A. B., J. Borel, A. Odone, S. Naidu, D. Cornblath, D. B. Sanders, and H. W. Moser. 1987. A new dietary therapy for adrenoleukodystrophy: biochemical and preliminary clinical results in 36 patients. *Ann. Neurol.* **21:** 240–249.
35. Rizzo, W. B., M. W. Phillips, A. L. Dammann, R. T. Leshner, S. S. Jennings, J. Avigan, and V. K. Proud. 1987. Adrenoleukodystrophy: dietary oleic acid lowers hexacosanoate levels. *Ann. Neurol.* **21:** 232–239.
36. Rizzo, W. B., R. T. Leshner, A. Odone, A. L. Dammann, D. A. Craft, M. E. Jensen, S. S. Jennings, S. Davis, R. Jaitly, and J. A. Sgro. 1989. Dietary erucic acid therapy for X-linked adrenoleukodystrophy. *Neurology.* **39:** 1415–1422.
37. Kaplan, P. W., R. J. Tusa, J. Shankroff, J. Heller, and H. W. Moser. 1993. Visual evoked potentials in adrenoleukodystrophy: a trial with glycerol trioleate and Lorenzo oil. *Ann. Neurol.* **34:** 169–174.

38. Odone, A., and M. Odone. 1989. Lorenzo's oil: a new treatment for adrenoleukodystrophy. *J. Pediatr. Neurosci.* **5:** 55–61.
39. Rasmussen, M., A. B. Moser, J. Borel, S. Khangoora, and H. W. Moser. 1994. Brain, liver, and adipose tissue erucic and very long chain fatty acid levels in adrenoleukodystrophy patients treated with glyceryl trierucate and trioleate oils (Lorenzo's oil). *Neurochem. Res.* **19:** 1073–1082.
40. Poulos, A., R. Gibson, P. Sharp, K. Beckman, and P. Grattan-Smith. 1994. Very long chain fatty acids in X-linked adrenoleukodystrophy brain after treatment with Lorenzo's oil. *Ann. Neurol.* **36:** 741–746.
41. Boles, D. J., and W. B. Rizzo. 1992. Dietary fatty acids temporarily alter liver very long chain fatty acid composition in mice. *J. Nutr.* **122:** 1662–1671.
42. Moser, H. W., G. V. Raymond, W. Koehler, P. Sokolowski, F. Hanefeld, G. C. Korenke, A. Green, D. J. Loes, D. H. Hunneman, R. O. Jones, et al. 2003. Evaluation of the preventive effect of glyceryl trioleate-trierucate ("Lorenzo's oil") therapy in X-linked adrenoleukodystrophy: results of two concurrent trials. *Adv. Exp. Med. Biol.* **544:** 369–387.
43. Moser, H. W., G. V. Raymond, S-E. Lu, L. R. Muenz, A. B. Moser, J. Xu, R. O. Jones, D. J. Loew, E. R. Melhem, P. Dubey, et al. 2005. Follow-up of 89 asymptomatic patients with adrenoleukodystrophy treated with Lorenzo's oil. *Arch. Neurol.* **62:** 1073–1080.
44. Ferri, R., and P. F. Chance. 2005. Lorenzo's oil: advances in the treatment of neurometabolic disorders. *Arch. Neurol.* **62:** 1045–1046.
45. Fraisl, P., S. Forss-Petter, M. Zigman, and J. Berger. 2004. Murine bubblegum orthologue is a microsomal very long-chain acyl-CoA synthetase. *Biochem. J.* **377:** 85–93.
46. Min, K-T., and S. Benzer. 1999. Preventing neurodegeneration in the *Drosophila* mutant *bubblegum*. *Science.* **284:** 1985–1988.
47. Robinson, P. J., J. Noronha, J. J. DeGeorge, L. M. Freed, T. Nariai, and S. I. Rapoport. 1992. A quantitative method for measuring regional in vivo fatty acid incorporation into and turnover within brain phospholipids: review and critical analysis. *Brain Res. Rev.* **17:** 187–214.
48. Chang, M. C., E. Grange, O. Rabin, J. M. Bell, D. D. Allen, and S. I. Rapoport. 1996. Lithium decreases turnover of arachidonate in several brain phospholipids. *Neurosci. Lett.* **220:** 171–174.
49. Chang, M. C. J., M. A. Contreras, T. A. Rosenberger, J. J. O. Rintala, J. M. Bell, and S. I. Rapoport. 2001. Chronic valproate treatment decreases the *in vivo* turnover of arachidonic acid in brain phospholipids: a possible common effect of mood stabilizers. *J. Neurochem.* **77:** 796–803.
50. Rosenberger, T. A., N. E. Villacreses, M. A. Contreras, J. V. Bonventre, and S. I. Rapoport. 2003. Brain lipid metabolism in the $cPLA_2$ knockout mouse. *J. Lipid Res.* **44:** 109–117.
51. Freed, L. M., S. Wakabayashi, J. M. Bell, and S. I. Rapoport. 1994. Effect of inhibition of (beta)-oxidation on incorporation of [U-(14)C]palmitate and [1-(14)C]arachidonate into brain lipids. *Brain Res.* **645:** 41–48.
52. Folch, J., M. Lees, and G. H. Sloane Stanley. 1957. A simple method for the isolation and purification of total lipides from animal tissues. *J. Biol. Chem.* **226:** 497–509.
53. Smith, B. S. 1970. A comparison of ^{125}I and ^{51}Cr for measurement of total blood volume and residual blood content of tissues in the rat: evidence for accumulation of ^{51}Cr by tissues. *Clin. Chim. Acta.* **27:** 105–108.
54. Rosenberger, T. A., J. Oki, A. D. Purdon, S. I. Rapoport, and E. J. Murphy. 2002. Rapid synthesis and turnover of brain microsomal ether phospholipids in the adult rat. *J. Lipid Res.* **43:** 59–68.
55. Radin, N. S. 1988. Lipid extraction. *In* Neuromethods 7: Lipids and Related Compounds. A. A. Boulton, G. B. Baker, and L. A. Horrocks, editors. Humana Press, Clifton, NJ. 1–62.
56. Jolly, C. A., T. Hubbell, W. D. Behnke, and F. Schroeder. 1997. Fatty acid binding protein: stimulation of microsomal phosphatidic acid formation. *Arch. Biochem. Biophys.* **341:** 112–121.
57. Marcheselli, V. L., B. L. Scott, T. S. Reddy, and N. G. Bazan. 1988. Quantitative analysis of acyl group composition of brain phospholipids, neutral lipids, and free fatty acids. *In* Neuromethods 7: Lipids and Related Compounds. A. A. Boulton, G. B. Baker, and L. A. Horrocks, editors. Humana Press, Clifton, NJ. 83–110.
58. Murphy, E. J., and F. Schroeder. 1997. Sterol carrier protein-2 mediated cholesterol esterification in transfected L-cell fibroblasts. *Biochim. Biophys. Acta.* **1345:** 283–292.
59. Wood, R., and T. Lee. 1983. High-performance liquid chromatography of fatty acids: quantitative analysis of saturated, monoenoic, polyenoic and geometrical isomers. *J. Chromatogr.* **254:** 237–246.
60. Chen, H., and R. E. Anderson. 1992. Quantitation of phenyl esters or retinal fatty acids by high-performance liquid chromatography. *J. Chromatogr.* **578:** 124–129.
61. Lee, H., N. E. Villacreses, S. I. Rapoport, and T. A. Rosenberger. 2004. *In vivo* imaging detects a transient increase in brain arachidonic acid metabolism: a potential marker of neuroinflammation. *J. Neurochem.* **91:** 936–945.
62. Singh, I., M. Khan, L. Key, and S. Pai. 1998. Lovastatin for X-linked adrenoleukodystrophy [letter]. *N. Engl. J. Med.* **339:** 702–703.
63. Singh, I., K. Pahan, and M. Khan. 1998. Lovastatin and sodium phenylacetate normalize the levels of very long chain fatty acids in skin fibroblasts of X-adrenoleukodystrophy. *FEBS Lett.* **426:** 342–346.
64. van Geel, B. M., J. Assies, E. B. Haverkort, J. H. T. M. Koelman, Jr., B. Verbeeten, R. J. A. Wanders, and P. G. Barth. 1999. Progression of abnormalities in adrenomyeloneuropathy and neurologically asymptomatic X-linked adrenoleukodystrophy despite treatment with "Lorenzo's oil." *J. Neurol. Neurosurg. Psychiatry.* **67:** 290–299.
65. Carroll, K. K. 1962. Levels of radioactivity in tissues and in expired carbon dioxide after administration of 1-C^{14}-labelled palmitic acid, 2-C^{14}-labelled erucic acid, or 2-C^{14}-labelled nervonic acid to rats. *Can. J. Biochem. Physiol.* **40:** 1229–1238.
66. Walker, B. L. 1972. Deposition of erucic acid in rat tissue lipids. *Nutr. Metab.* **14:** 8–16.
67. Rapoport, S. I., M. C. J. Chang, and A. A. Spector. 2001. Delivery and turnover of plasma-derived essential PUFAs in mammalian brain. *J. Lipid Res.* **42:** 678–685.
68. Augustus, A. S., Y. Kako, H. Yagyu, and I. J. Goldberg. 2003. Routes of FA delivery to cardiac muscle: modulation of lipoprotein lipolysis alters uptake of TG-derived FA. *Am. J. Physiol.* **284:** E331–E339.
69. Teusink, B., P. J. Voshol, V. E. H. Dahlmans, P. C. N. Rensen, H. Pihl, J. A. Romijn, and L. M. Havekes. 2003. Contribution of fatty acids released from lipolysis of plasma triglycerides to total plasma fatty acid flux and tissue-specific fatty acid uptake. *Diabetes.* **52:** 614–620.
70. Zhao, M., and K. H. Muntz. 1993. Differential downregulation of β_2-adrenergic receptors in tissue compartments of rat heart is not altered by sympathetic denervation. *Circ. Res.* **73:** 943–951.